TOXICOLOGICAL SCIENCES **136(2)**, 500–513 2013
doi:10.1093/toxsci/kft202
Advance Access publication September 7, 2013

Structure-Activity Relationship of Selected *Meta*- and *Para*-Hydroxylated Non–Dioxin Like Polychlorinated Biphenyls: From Single RyR1 Channels to Muscle Dysfunction

Yassaman Niknam,* Wei Feng,* Gennady Cherednichenko,* Yao Dong,* Sudhir N. Joshi,† Sandhya M. Vyas,† Hans-Joachim Lehmler,† and Isaac N. Pessah*,‡,[1]

*Department of Molecular Biosciences, School of Veterinary Medicine, University of California, Davis, California 95616; †Department of Occupational and Environmental Health, College of Public Health, University of Iowa, Iowa City, Iowa 52242; and ‡The Medical Investigation of Neurodevelopmental Disorders (MIND) Institute, University of California at Davis, Sacramento, California 95817

[1]To whom correspondence should be addressed at Department of Molecular Biosciences, School of Veterinary Medicine, University of California, 1089 Veterinary Medicine Drive, Davis, CA 95616. Fax: 530-752-4698. E-mail: inpessah@ucdavis.edu.

Received June 15, 2013; accepted August 29, 2013

Non–dioxin like polychlorinated biphenyls (NDL-PCBs) are legacy environmental contaminants with contemporary unintentional sources. NDL-PCBs interact with ryanodine receptors (RyRs), Ca^{2+} channels of sarcoplasmic/endoplasmic reticulum (SR/ER) that regulate excitation-contraction coupling (ECC) and Ca^{2+}-dependent cell signaling in muscle. Activities of 4 chiral congeners PCB91, 95, 132, and 149 and their respective 4- and 5-hydroxy (-OH) derivatives toward rabbit skeletal muscle ryanodine receptor (RyR1) are investigated using [^{3}H]ryanodine binding and SR Ca^{2+} flux analyses. Although 5-OH metabolites have comparable activity to their respective parent in both assays, 4-OH derivatives are unable to trigger Ca^{2+} release from SR microsomes in the presence of Ca^{2+}-ATPase activity. PCB95 and derivatives are investigated using single channel voltage-clamp and primary murine embryonic muscle cells (myotubes). Like PCB95, 5-OH-PCB95 quickly and persistently increases channel open probability ($p_o > .9$) by stabilizing the full-open channel state, whereas 4-OH-PCB95 transiently enhances p_o. Ca^{2+} imaging of myotubes loaded with Fluo-4 show that acute exposure to PCB95 (5μM) potentiates ECC and caffeine responses and partially depletes SR Ca^{2+} stores. Exposure to 5-OH-PCB95 (5 μM) increases cytoplasmic Ca^{2+}, leading to rapid ECC failure in 50% of myotubes with the remainder retaining negligible responses. 4-OH-PCB95 neither increases baseline Ca^{2+} nor causes ECC failure but depresses ECC and caffeine responses by 50%. With longer (3 h) exposure to 300nM PCB95, 5-OH-PCB95, or 4-OH-PCB95 decreases the number of ECC responsive myotubes by 22%, 81%, and 51% compared with control by depleting SR Ca^{2+} and/or uncoupling ECC. NDL-PCBs and their 5-OH and 4-OH metabolites differentially influence RyR1 channel activity and ECC in embryonic skeletal muscle.

Key Words: **calcium signaling; ryanodine receptor; muscle dysfunction; polychlorinated biphenyls; hydroxylated metabolites.**

Polychlorinated biphenyls (PCBs), banned in the 1970s, still persist at high concentrations in the environment and in animal and human tissues including liver, brain, fat, blood, and skeletal muscle (Pessah *et al.*, 2010). Recently, PCB mixtures have been identified in elementary schools (Thomas *et al.*, 2012) where *ortho*-substituted non–dioxin like PCB congeners (NDL-PCB) that lack activity toward the aryl hydrocarbon receptor (AhR) predominate. For example, PCB95 (2,2′,3,5′,6-pentachlorobiphenyl), a developmental neurotoxicant (Kenet *et al.*, 2007; Schantz *et al.*, 1997; Yang *et al.*, 2009), is the second most abundant congener found in indoor/outdoor air, soil, and caulking found in New York City schools (Thomas *et al.*, 2012). Contemporary unintentional sources of NDL-PCBs, including PCB95, from the paint pigment industry have been identified (Hu and Hornbuckle, 2010).

Although the focus of scientific studies has been on dioxin-like PCBs, neurotoxicity and endocrine disruption appear to be independent of AhR interactions (Pessah *et al.*, 2010). NDL-PCBs with 2 or more *othro*-chlorines contribute > 50% of the PCB burden in both environmental samples and human tissues, such as those individuals near the Great Lakes, St Lawrence River, and Fox River (DeCaprio *et al.*, 2005; Kostyniak *et al.*, 2005; Marek *et al.*, 2013; Martinez and Hornbuckle, 2011; Martinez *et al.*, 2012). A molecular target through which NDL-PCBs could mediate a broad cadre of toxicological sequelae stems from interactions with ryanodine receptors (RyRs) that form Ca^{2+} channels that mediate the highly controlled release of Ca^{2+} from sarcoplasmic/endoplasmic reticulum (SR/ER) stores to the cytoplasm (Pessah *et al.*, 2010). Three RyR isoforms are broadly expressed in c ells with the type 1 isoform RyR1 being one of two Ca^{2+} channels essential for excitation-contraction coupling (ECC) in mammalian skeletal muscle, the other being

the L-type voltage-gated Ca^{2+} channel CaV1.1 (Nakai *et al.*, 1996; Tanabe *et al.*, 1988).

Behavioral, cognitive, and motor impairments have been associated with PCB exposure and attributed to their ability to alter critical neurodevelopmental milestones in the central nervous system (CNS) such as activity-dependent dendritic growth (Wayman *et al.*, 2012a,b; Yang *et al.*, 2009). However, little attention has been given to striated muscle as a potential target organ. In humans, prenatal exposure to PCBs has been associated with lower body weight, consistent with decreased total lean body mass reported for children born to mothers accidentally exposed to PCBs (Coletti *et al.*, 2001), which was not due to decreased bone density or body fat. In addition, rat myogenic cultures exposed to PCB mixture Aroclor 1254 *in vitro* inhibited myoblast differentiation (Guo *et al.*, 1994). These results indicate that in addition to developmental neurotoxicity mediated by interactions of NDL-PCB with RyRs expressed in the CNS (Pessah *et al.*, 2010), direct actions with RyR1 expressed in skeletal muscle could contribute to motor dysfunction, especially during critical perinatal periods of muscle development.

There is increasing interest in whether metabolites of NDL-PCBs maintain biological activity. Cytochrome P450 monooxygenase enzymes (CYP) metabolize PCBs to their respective OH-PCB (Warner *et al.*, 2009). OH-PCBs can be more reactive toward biological targets and contribute to toxicity (Song *et al.*, 2013), especially because they are retained in blood (Hovander *et al.*, 2002). Pharmacokinetic studies indicate PCBs initially distribute to muscle where OH-PCBs may be locally formed by CYPs expressed in skeletal muscle (Bièche *et al.*, 2007; Kania-Korwel *et al.*, 2007). PCB metabolites can persist in plasma at concentrations 15-fold higher than their parent compound, making them long-lasting environmental and biological contaminants (Bergman *et al.*, 1994; Larsson *et al.*, 2002; Lehmler *et al.*, 2010).

In this report, we provide direct evidence that OH-PCBs interact with RyR1 of skeletal muscle and produce a differential pattern of single channel gating kinetics and myotube ECC dysfunction that is highly dependent on whether the 4- or 5-position is hydroxylated. Direct impairment of muscle Ca^{2+} dynamics and function may explain, at least in part, the impairments in skeletal muscle health observed in human and animal studies.

MATERIALS AND METHODS

Reagents and chemicals. Parent PCB congeners (91, 95, 132, and 149) were purchased as neat standards (> 99%) from AccuStandard (New Haven, CT) and dissolved in dry dimethyl sulfoxide (DMSO) to 10 mM and stored at −80°C. The hydroxylated PCB derivatives were synthesized and characterized as described previously (Joshi *et al.*, 2011). The chemical structures and abbreviations of all PCB derivatives used in the present study are shown in Figure 1. 4-OH-PCB 149 was not synthesized and therefore was not available for testing were synthesized and characterized as described previously (Joshi *et al.*, 2011). 4-OH-PCB149 was not synthesized and therefore was not available for testing. The chemical structures used in this study are shown in Figure 1.

SR membrane preparations. Microsomal membrane vesicles from junctional SR and enriched in RyR1 were isolated from fast-twitch (white) skeletal muscles obtained from the back of 1-year-old male (2–2.5 kg) New Zealand White rabbits, as previously described (Pessah *et al.*, 1987; Saito *et al.*, 1984).

Tritium-labeled ryanodine binding assay. Tritium-labeled ryanodine ([^{3}H]Ry; 95 Ci/mmol) was purchased from PerkinElmer (Santa Clara, California). Specific binding of [^{3}H]Ry to isolated skeletal muscle microsomes was performed as previously reported (Pessah *et al.*, 1985, 1987). Each experiment was performed in triplicate ($n = 3$) and replicated at least twice. The free Ca^{2+} concentration in the assay buffer was adjusted to promote the open state of the RyR1 channel activity (50 µM Ca^{2+}) or promote a less active channel state (1 µM Ca^{2+}) by addition of ethylene glycol-bis(2-aminoethylether)-*N,N,N′,N′*-tetraacetic acid (EGTA) based on the Bound and Determined program (Brooks and Storey, 1992).

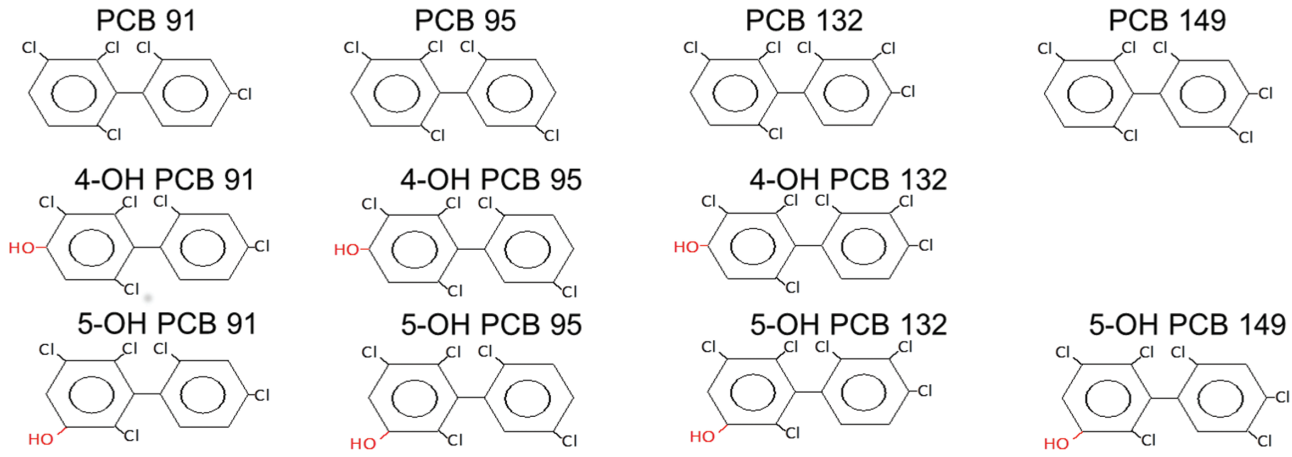

FIG. 1. Structures of NDL-PCBs and their respective hydroxylated derivatives. PCB91 (2,2′,3,4′,6-pentachlorobiphenyl); PCB95 (2,2′,3,5′,6-pentachlorobiphenyl); PCB132 (2,2′,3,3′,4,6′-hexachlorobiphenyl); PCB149 (2,2′,3,4′,5′,6-hexachlorobiphenyl). 4-OH-PCB149 was not available for testing. Abbreviation: NDL-PCBs, non–dioxin like polychlorinated biphenyls.

Macroscopic Ca^{2+} flux measurement. Net Ca^{2+} efflux from isolated skeletal SR microsomes was measured with the metallochromic Ca^{2+}-sensitive dye antipyrylazo III (APIII) as previously described (Pessah *et al.*, 2006, 2009). Briefly, active Ca^{2+} loading into microsomal vesicles was performed by energizing the SR/ER Ca^{2+} ATPase (SERCA) pump using ATP hydrolysis enzymatically coupled to ATP synthesis with phosphocreatine and creatine phosphokinase. Vesicles were loaded by sequential additions of approximately 50 nM of Ca^{2+} until Ca^{2+} uptake neared the capacity of the vesicles. Ca^{2+} release was tested by the subsequent addition of 10 µM NDL-PCB or derivative or addition of an equivalent volume of solvent (DMSO) that served as the vehicle control. In experiments aimed at testing the mechanism of PCB-triggered Ca^{2+} release, the RyR1 inhibitor ruthenium red (RR, 1 µM) was injected into the cuvette immediately after Ca^{2+} loading was complete and incubated for an extra 100 s prior to addition of PCB. Each compound was tested 2–3 times in at least 2 different microsomal preparations.

Measurements of RyR1 single channel activity in bilayer lipid membrane. Single channel recordings and data analysis were carried out as previously described (Pessah *et al.*, 2009; Samsó *et al.*, 2009). Briefly, a bilayer lipid membrane (BLM) was formed at 30 mg/ml phosphatidylethanolamine/phosphatidylserine/phosphatidylcholine in decane (Avanti, Alabaster, Alabama). A Cs^+ gradient was built from *cis* to *trans* (500 to 50 mM of CsCl) in 20 mM Hepes, pH of 7.4. The holding potential of –40 mV was applied to the *trans* (ground) side versus *cis*. SR vesicles, the test compounds, and defined Ca^{2+} were added in the *cis* chamber as reported in the figure legend, whereas *trans* was held consistently at 100 µM Ca^{2+}. Once channel reconstitution was obtained, the *cis* chamber was perfused to prevent additional fusions. Fusions using this method consistently oriented the cytoplasmic face of the channel toward the *cis* chamber and the luminal side of the channel facing the *trans* chamber. Baseline recording of channel gating behavior was acquired for 400 s under defined *cis/trans* conditions. Vehicle, NDL-PCB, or metabolite was added (10 µM) and data acquired for at least 5 min. Data acquisitions and analysis for channel open probability (p_o) and open (τ_o) and closed (τ_c) dwell times were performed with software pClamp 10.2 (Molecular Devices, California).

Preparation of primary myotubes and single cell Ca^{2+} imaging. The UC Davis Animal Use Committee approved all experimental uses of animals. Primary skeletal myoblasts were isolated from newborn (postnatal day 1–2) wild-type C57bl/6 mice as previously described (Cherednichenko *et al.*, 2008). The myoblasts were expanded in 10-cm cell culture–treated Corning dishes coated with collagen and were plated onto 96-well µ-clear plates (BD Falcon) coated with Matrigel (BD Biosciences) in the presence of 20% fetal bovine serum (FBS) and basic fibroblast growth factor (bFGF). Upon reaching approximately 80% confluence, FBS and bFGF were substituted with 5% heat-inactivated horse serum in Dulbecco's Modified Eagle's Medium to promote cell differentiation into myotubes over a period of 3–5 days for Ca^{2+} imaging studies. Myotubes were loaded with the Ca^{2+} indicator Fluo-4 (5 µM) for 20 min in imaging buffer composed of 146 mM NaCl, 5 mM KCl, 0.6 mM $MgSO_4$, 6 mM glucose, 25 mM HEPES, and 2 mM $CaCl_2$ and 0.5 mg/ml bovine serum albumin. Cells were rinsed to remove external dye. Plates were placed on the stage of an inverted microscope equipped with 40× objective (Nikon, Melville, New York), illuminated at 494 nm using a DeltaRam (PTI) wavelength-selectable light source to excite Fluo-4, and imaged at 516 nm with a cooled CCD camera (Cascade 512B). Electrical field stimuli were applied using 2 platinum electrodes that were fixed to opposing sides of the well and connected to A.M.P.I. Master 8 stimulator set at 7 V, 1-ms bipolar pulse duration over 1–40 Hz (10-s pulse train duration). After each stimulation epoch, cells were allowed to rest for 35–50 s.

Two exposure protocols were used after testing baseline functional responses described above: (1) Acute (10 min) exposure of myotubes to 5 µM NDL-PCBs (PCB95, 5-OH-PCB95, or 4-OH-PCB95) during which time cells were continuously stimulated at 0.1 Hz. Following a recovery period, the cells were challenged with the same electrical pulse train protocol described above to assess changes in Ca^{2+}-transient amplitudes and responses to 20 mM caffeine at the end of the experiment. In separate experiments aimed at assessing the filling state of SR Ca^{2+} stores after acute exposure to NDL-PCBs, cells were challenged with 400 nM thapsigargin (TG), an irreversible SERCA inhibitor, in Ca^{2+}-free extracellular buffer. (2) Subacute (3 h) exposure of myotubes to 250–300 nM NDL-PCBs was performed in a serum-free medium at 37°C in a tissue culture incubator, subsequently loaded with Fluo-4, and imaged as described above, while maintaining the concentration of NDL-PCB throughout each step. Functional responses from individual cells to electrical pulse trains (1–40 Hz) and caffeine were tested as described above for the acute study. Each well containing myotubes was analyzed for a total number of cells responding to 1 Hz in 3–5 different randomly chosen fields. Ca^{2+} transients were normalized to baseline (F_o) of each cell and corrected for background. The images were acquired using the Easy Ratio Pro Software (PTI), and data were then analyzed using Origin 8.5 software (OriginLab Corp., Northampton, Massachusetts) and Graphpad Prism 5 software. All experiments were replicated at least thrice in 3–5 different passages (n = 3–5).

Data analysis. Concentration-effect curves were fit with a nonlinear regression equation using Origin 8.5 software (OriginLab Corp.) as described previously (Pessah *et al.*, 2006). Two parameters were calculated: (1) the concentration needed to obtain 50% of the maximal receptor activity (EC_{50}) and (2) the maximal receptor activity normalized to control at 100% (% maximum response from control). The rate of Ca^{2+} release induced by selected PCBs was determined by linear regression analysis of Ca^{2+} release after the initial lag phase of Ca^{2+} efflux (all r^2 values ≥ .9). All analyses were compared with each treatment's respective control (0.1% DMSO). Imaging data were analyzed using GraphPad Prism5 Software. Normalized amplitudes were calculated as $\Delta F/F_o$ after electrical stimulation and 20 mM caffeine challenge. Data were analyzed using a one-way ANOVA with Dunnett's *post hoc* test. $^*p < .05$; $^{**}p < .01$; $^{***}p < .001$.

RESULTS

[^{3}H]Ry-Binding Analysis Identifies Divergent Activities of 5-OH and 4-OH NDL-PCBs

To determine whether 5-OH or 4-OH substitutions confer differences in activity toward RyR1 relative to their respective parent compound, we investigated the structure-activity relationship (SAR) for 4 chiral NDL-PCB congeners using [^{3}H]Ry binding analysis. Parent compounds and their –OH derivatives were tested as racemic mixtures. Nanomolar [^{3}H]Ry binds preferentially to specific sites that are unmasked when the RyR1 channel complex is in a conducting (open) state and therefore can be used as biochemical indicator of ligand-mediated shifts in RyR1 channel conformation (Pessah *et al.*, 1987). Under the experimental conditions used, all NDL-PCBs tested showed monotonic concentration-effect curves but differed in apparent potencies (EC_{50}) and efficacies (maximum (Max) binding) for enhancing [^{3}H]Ry-binding to RyR1 at steady state (3-h incubation) (Fig. 2A). Table 1 summarizes the EC_{50} parameter (in micromoles), with parent compounds showing a rank order of PCB95 < PCB149 < PCB91 ~ PCB132, whereas the rank efficacy was PCB95 > PCB132 ~ PCB149 > PCB91. The concentration-effect relationships for both 5-OH- and 4-OH-PCB95 differ significantly ($p < .01$) from that of PCB95 (Fig. 2B). The 5-OH substitution did not significantly influence the EC_{50} relative to PCB95 but did increase maximum binding nearly 30% ($p < .01$), reaching nearly 10-fold baseline (Table 1). By contrast, 4-OH-PCB95 showed lower apparent potency ($p < .001$) and a tendency for lower efficacy toward RyR1 activation than

the parent compound (Fig. 2B; Table 1). For the congeners tested, the general tendency indicated that 5-OH substitution maintained or improved potency and/or efficacy compared with their parent compound, whereas 4-OH substitution was not as active toward RyR1 when [^{3}H]Ry was used as readout for channel function (Table 1). Note: The same PCB95 representative traces are used in Figures 2A, 2B, 3A, and 3B.

5-OH-PCBs, But Not 4-OH-PCBs, Trigger Ca^{2+} Efflux From SR With SERCA Activity

To determine whether the SAR results from [^{3}H]Ry-binding analysis predict the ability of NDL-PCBs to trigger Ca^{2+} efflux from SR vesicles, each congener was introduced at the highest concentration tested (10 µM) into a spectrophotometric cuvette containing SR vesicles loaded with Ca^{2+} using ATP-driven SERCA activity, which is abundant in these preparations, as described in Materials and Methods section. Once the PCB derivative was introduced into the cuvette, the rate and extent of Ca^{2+} release into the extravesicular buffer were monitored in real time. The results shown in Figure 3A indicated that the rate of PCB-triggered Ca^{2+} release differed by congener and showed a rank order of PCB95 > PCB91 > PCB149 > PCB132 (Fig. 3C). PCB95, PCB132, and PCB149 released nearly all of the Ca^{2+} accumulated in the loading phase of the experiment, whereas PCB91 only caused partial release of accumulated Ca^{2+}, reaching a new steady state after

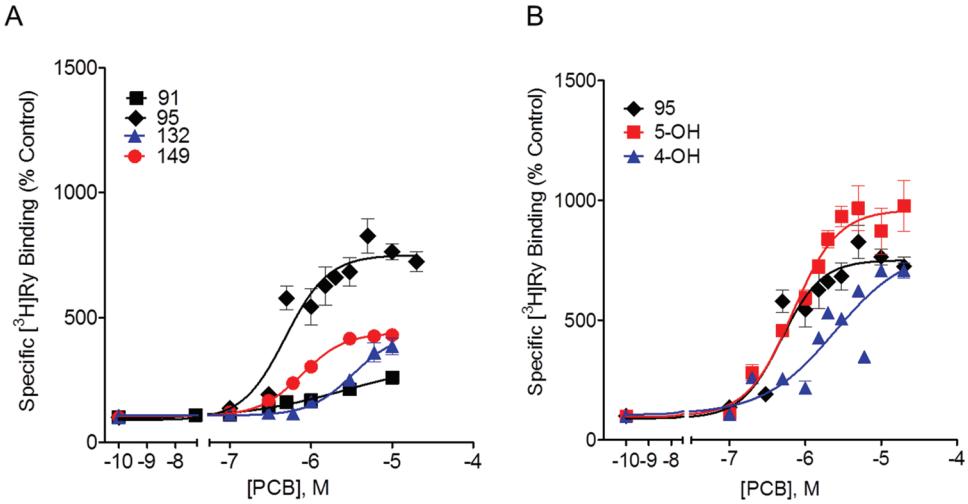

FIG. 2. Chiral NDL-PCBs and their hydroxylated derivatives enhance [^{3}H]Ry binding in a concentration-dependent manner. A, Concentration-effect curves for enhancing the specific binding of [^{3}H]Ry by 4 racemic NDL-PCBs. Equilibrium binding of [^{3}H]Ry to RyR1 was performed in the absence and presence (0–20 µM) of PCB91 (91), PCB95 (95), 5-OH-PCB95 (5-OH), 4-OH-PCB95 (4-OH), PCB132 (132), or PCB149 (149) as described in the Materials and Methods section. The potency and efficacy are summarized in Table 1. B, Concentration-effect relationship for enhancing the specific binding of [^{3}H]Ry by 4-OH- and 5-OH-PCB95 relative to their parent congener PCB95. The binding experiment was repeated in triplicates in at least 2 different tissue preparations, and the averaged results are shown in the figures. Baseline DPM ranged from 1000 to 1500 DPM. *Note*. The same PCB95 trace was used in both panels (A) and (B). Abbreviation: NDL-PCBs, non–dioxin like polychlorinated biphenyls.

TABLE 1
SAR Resulting From [^{3}H]Ry Binding Analysis of 4 NDL-PCBs and Their 5-OH and 4-OH derivatives

	EC_{50} (µM)[a]			95% Confidence Interval			Max Binding (% Control)[b]		
Congener	Parent PCB	5-OH	4-OH	Parent PCB	5-OH	4-OH	Parent PCB	5-OH	4-OH
91	2.71	3.73	3.67	1.14–6.47	2.31–6.02	0.70–19	324 ± 27	377 ± 22	233 ± 10***
95	0.49	0.68	2.46***	0.34–0.68	0.34–0.89	0.89–6.76	750 ± 33	960 ± 42**	707 ± 131
132	3.33	5.37[c]	3[c]	1.70–6.52	[c]	[c]	442 ± 68	540[c]	241[c]
149	0.77	2.14***	NA	0.64–0.93	1.67–2.75	NA	439 ± 11	647 ± 10***	NA

Note. The potency and efficacy of select PCB congeners toward enhancing [^{3}H]Ry binding were analyzed as described in the Materials and Methods section.

[a]Data show averages and SEs for [PCB] needed to enhance specific [^{3}H]Ry binding to half of the maximum (EC_{50}). NA are compounds that were not available to be tested.

[b]Data were calculated as % of baseline specific binding measures in the absence of PCB (ie, % control), where all responses were compared to a baseline of 100%; maximal responses were recorded to their respective controls. Errors represent SEM.

[c]Data ≤ 20 µM did not converge on Max under the assay conditions tested; therefore, EC_{50} and Max values are estimates obtained without curve fitting (ie, Max value at 20 µM and concentration need to obtain 50% of Max).

$^{**}p < .01$; $^{***}p < .001$.

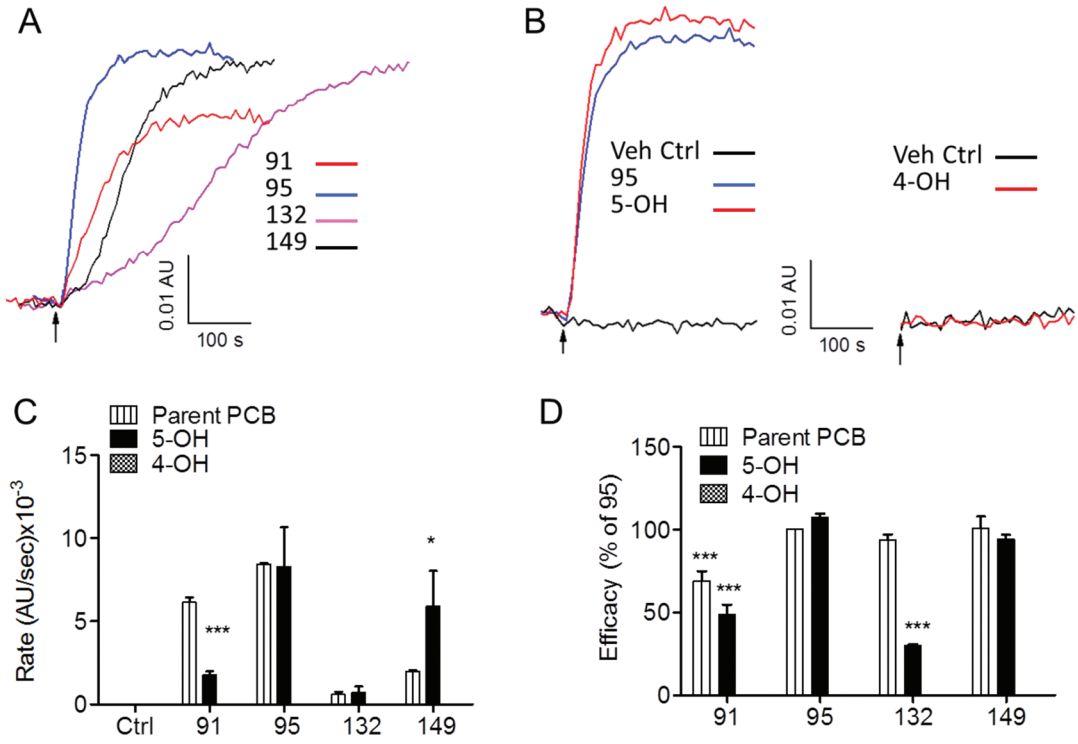

FIG. 3. NDL-PCBs and their 5-OH derivatives trigger Ca^{2+} release from skeletal SR. A, Representative traces of Ca^{2+} efflux from skeletal SR membrane vesicles triggered by addition of 4 NDL-PCBs; arrow represents addition of a saturating concentration (10 µM) of each PCB. B, Representative traces of Ca^{2+} release triggered by 10 µM PCB95 and 5-OH-PCB95 (arrow). Right panel shows that 4-OH-PCB95 failed to trigger Ca^{2+} release from the SR vesicles. C, Summary of rate of Ca^{2+} efflux mediated by RyR1 activation (AFU abs/sec) by PCB91, PCB95, PCB132, PCB149, and their 5-OH-derivatives. None of the 4-OH-derivatives tested released Ca^{2+} from the SR vesicles under the experimental conditions used (see Materials and Methods section). Rates were recorded as changes in arbitrary absorbance units per second, and the bars indicate the mean ± SE of $n = 3$ experiments using at least 2 different SR membrane preparations. D, The total amount of Ca^{2+} released from SR vesicles by each NDL-PCB presented as percent of PCB95 (considered a full allosteric RyR1 enhancer). $*p < .05$; $***p < .001$, unpaired *t* test (comparison of compounds to respective parent PCB); all compounds (excluding 4-OH metabolites) were significantly higher than vehicle control; $***p < .001$; one-way ANOVA with *Dunnett multiple comparison post hoc* test. *Note.* The same PCB95 trace was used in both panels (A) and (B). Abbreviations: NDL-PCBs, non–dioxin like polychlorinated biphenyls; SR, sarcoplasmic reticulum.

45%–55% of the stored Ca^{2+} was released into the extravesicular buffer (Figs. 3A and D), indicating lower efficacy. PCB95 and 5-OH-PCB95 revealed similar rates and amounts of Ca^{2+} release from SR vesicles (Fig. 3B, left panel) and were the most efficacious congeners tested (Figs. 3C and D). Figure 3B (right panel) showed that unlike PCB95 or 5-OH-PCB95, addition of 4-OH-PCB95 failed to produce net Ca^{2+} efflux under these experimental conditions. In fact, none of the 4-OH-PCBs tested were capable of triggering the release of Ca^{2+} from SR vesicles in the presence of SERCA pump activity (Figs. 3C and D). The rate and amount of Ca^{2+} release were highly congener dependent. 5-OH-PCB91 was overall less active than its parent congener, whereas 5-OH-PCB149 caused a faster initial rate of Ca^{2+} release than PCB149 and showed similar efficacy. By contrast, 5-OH-PCB132 triggered a similar initial rate of Ca^{2+} release but had significantly lower efficacy than PCB132 (Figs. 3C and D). PCB- and OH-PCB-triggered Ca^{2+} efflux from SR vesicles was mediated by selective activation of RyR1 channel activity because prior addition of RR, a known blocker of RyR channels, invariably prevented Ca^{2+} release (not shown).

5-OH- and 4-OH-PCB95 Differentially Alter RyR1 Channel Gating Properties

Previously, we showed that PCB95 stabilized the full-open state of the purified RyR1/FKBP12 complex reconstituted in the BLM preparation to define direct structure-function relationships at the level of single channels (Samsó *et al.*, 2009). Here we used the same BLM approach and tested how 5-OH- and 4-OH-PCB95 would alter RyR1 single channel current gating properties under voltage clamp conditions. The gating RyR1 single channel in the presence of 50 µM *cis* (cytoplasmic) Ca^{2+} was recorded before (for 1–2 min as control) and after introducing PCB to the *cis* side of the reconstituted channel. Representative diary plots showing continuous recordings of open probability (p_o) over the entire time course of representative experiments before and after additions of either 5-OH-PCB95 or 4-OH-PCB95 are summarized in Figure 4A (right panel). Under the *cis/trans* conditions used to measure channel current gating activity, the baseline open probability (p_o) averaged approximately 0.26 in $n = 9$ channel reconstitutions (Fig. 4B, Control column I). Addition of 5-OH-PCB95 to the *cis* chamber rapidly stabilized the full open (conducting)

A

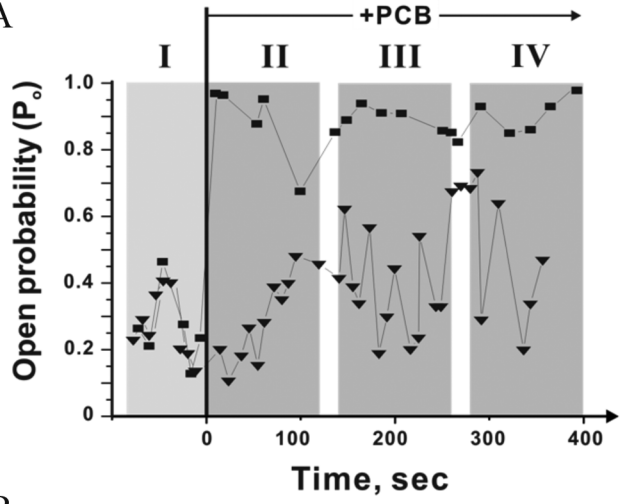

Ex. group	Control	PCB		
	I	II	III	IV
■	Ca^{2+}, 50μM	5-OH (10μM)		
▼	Ca^{2+}, 50μM	4-OH (10μM)		

B

Experiment group (Channel gating parameters)		Control I	PCB II	PCB III	PCB IV
■ 5-OH (10μM)	Po	0.263 ± 0.112	0.864 ± 0.116***	0.893 ± 0.038***	0.901 ± 0.043***
	Mean open time (ms)	0.82 ±0.21	8.68 ± 6.45***	6.38 ± 1.96***	6.03 ± 1.98***
	Mean closed time (ms)	2.15 ± 0.43	1.10 ± 0.43*	0.69 ± 0.12**	0.59 ± 0.085**
▼ 4-OH (10μM)	Po	0.268 ± 0.010	0.298 ± 0.127	0.397 ± 0.161	0.479 ± 0.211*
	Mean open time (ms)	0.88 ± 0.26	1.06 ± 0.41	1.49 ± 0.79	1.90 ± 0.96**
	Mean closed time (ms)	2.38 ± 0.65	2.46 ± 0.73	1.98 ± 0.65	2.06 ± 1.015

FIG. 4. 4-OH-PCB95 (4-OH) and 5-OH-PCB95 (5-OH) differentially alter RyR1 single channel gating activity. Current gating activities of RyR1 single channels reconstituted in BLM before and after exposure to 10 μM 5-OH-PCB95 (5-OH) or 4-OH-PCB95 (4-OH) were recorded in the presence of 50 μM *cis* (cytoplasmic side) Ca^{2+} at a holding potential of −40 mV (applied to the *trans* [luminal side] of the channel as described in Materials and Methods section). A, Open probability (p_o) diary plot that depicts the continuous time course of *p*o changes before (Stage I) and after PCB addition (Stages II, III, and IV) to the *cis* side of the RyR1 channel (left panel). Right panel summarizes the composition of the cytoplasmic Ca^{2+} and PCB concentrations used in the experimental protocol. B, Data were sampled in 2 s epochs and taken at 8–30 s intervals to calculate p_o, mean open dwell time (t_o, ms), and mean closed dwell time (t_c, ms) to obtain summary table containing mean values of channel gating parameters at each stages: stage I, Control basal channel activity, and after OH-PCB addition stages II, III, and IV. C and D, Representative channel current traces before and after exposure to OH-PCB taken from each time course stage (I–IV). The arrows with "O" and "C" indicate the current amplitudes of the channel at fully open and closed states, respectively. Consistent responses under the identical recording conditions were observed in $n = 6$ and $n = 3$ independent BLM measurements for 5-OH and 4-OH, respectively. Statistical analysis results are indicated as $*p < .05$; $**p < .01$; $***p < .001$, between control (basal channel activity—Stage I) and after addition of PCB at Stage II through IV. Abbreviations: BLM, bilayer lipid membrane; PCB, polychlorinated biphenyl.

state of the channel, attaining very high p_o (> .9) for the duration of these experiments (Figs. 4A and B, PCB Sections II–IV squares). The high p_o resulted from extremely long-lived channel openings (open dwell times from 0.8 ms at baseline to > 6 ms) and shortened mean closed dwell times (from > 2 ms at baseline to < 0.6 ms; Fig. 4B). These effects of 5-OH-PCB95 were nearly identical to those previously reported with PCB95 (Samsó *et al.*, 2009). By contrast, 4-OH-PCB95 added to the *cis* chamber increases channel p_o more slowly, reaching a p_o of .479 ± .211 at the end of phase IV, Figs. 4A and B). Importantly, the temporal stability of the 4-OH-PCB95 modified RyR1 channels was transient, showing significant fluctuations back to the original baseline p_o during phases III and IV of the recordings (Fig. 4A, triangles). Representative single channel traces shown in Figures 4C and 4D clearly differentiate modifications of gating behavior imposed by the presence 5-OH-PCB95 and 4-OH-PCB95.

PCB Substitution Determines Pattern of Acute Myotube ECC Dysfunction

Because of the dramatic SAR observed in the results from mechanistic studies presented above, we further investigated whether PCB95 and its 5- and 4-OH derivatives differ in their influence on Ca^{2+} dynamics and ECC in primary myotubes during an acute (10–15 min) exposure. Introduction of either vehicle (Ctrl) or PCB95 (5 μM) into the myotubes perfusion buffer did not alter the fraction of ECC responsive myotubes, whereas unexpectedly, 50% of myotubes exposed to 5-OH-PCB95 failed to respond at all frequencies tested (1–20 Hz) within 10 min (Table 2, $p < .01$). Acute exposure to 4-OH-PCB95

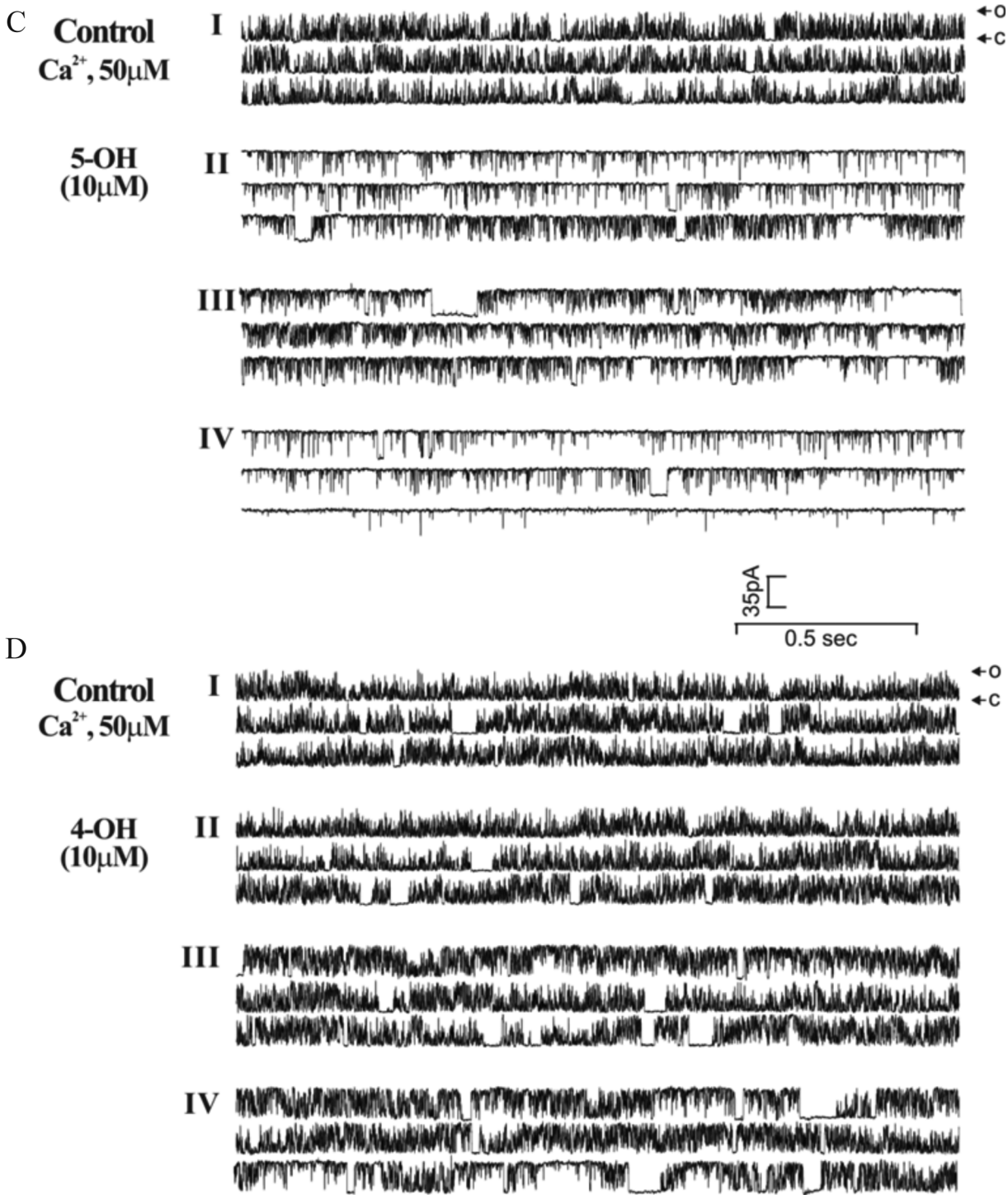

FIG. 4. Continued.

caused a modest, but statistically insignificant, decrease in the number of ECC responsive myotubes at stimulus frequencies < 10 Hz (Table 2).

However, myotubes maintaining ECC responses in the presence of these PCB95, 5-OH-PCB95, and 4-OH-PCB95 showed marked qualitative and quantitative differences in their basal Ca^{2+} regulation and in ECC compared with myotubes under control conditions (Fig. 5, upper right panel). Acute exposure to PCB95 potentiated Ca^{2+}-transient amplitude at low (1 Hz) stimulus frequency ($p < .05$) and had a tendency for smaller, though not significant, responses at ≥10 Hz stimulus frequencies (Figs. 5A [lower left panel] and 5B [diamonds]). Both 5-OH- and

TABLE 2
Percentage of Cells Responding to Electrical Stimulation in the Presence and Absence of 5 µM PCB95 (95), 5-OH-PCB95 (5-OH), or 4-OH-PCB95 (4-OH)

Congener	1 Hz	2.5 Hz	5 Hz	10 Hz	20 Hz	Caff
Control	100	100	100	100	100	100
95	100	100	100	100	100	100
5-OH	50±22**	50±23**	50±23**	50±23***	50±23***	96±4
4-OH	85±15	83±17	89±11	100	100	100

Note. Complete failure was defined as no detectable Ca^{2+} transients in response to electrical stimulation.
**$p < .01$; ***$p < .001$ unpaired t test.

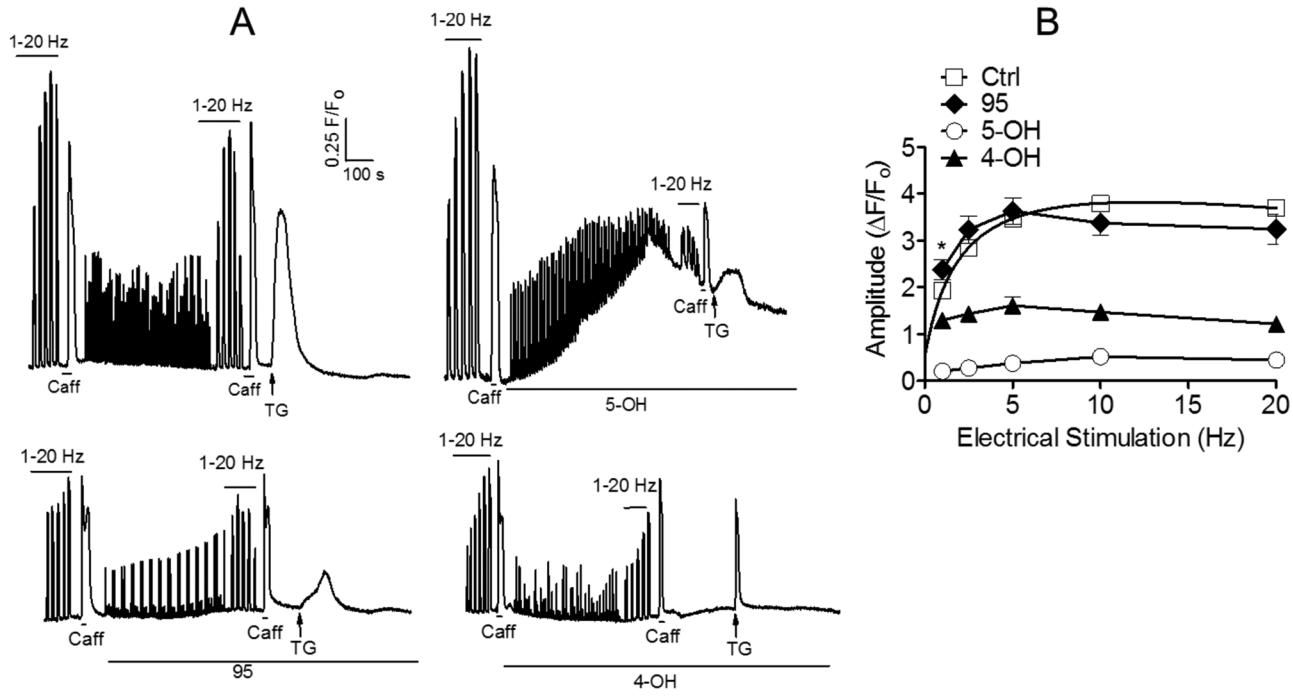

FIG. 5. PCB95, 4-OH-PCB95, and 5-OH-PCB95 elicit different patterns of impairment of electrically evoked ECC. A, Myotubes loaded with the Fluo-4 where individually imaged to measure changes in their cytoplasmic Ca^{2+} in response to electrical stimuli (1–20 Hz) and a short (10 s) bolus of Caff as described in Materials and Methods. Traces shown are representative responses before and after vehicle (upper left panel), 5 µM PCB95 (95; lower left panel), 5 µM 5-OH-PCB95 (5-OH; upper right panel), or 5 µM 4-OH-PCB95 (4-OH; lower right panel). At the end of each experiment, TG (400 nM) was added to irreversibly inhibit SERCA pump activity and assess the filling state of the SR Ca^{2+} store. B, Mean frequency-response curves from myotubes after exposure to Ctrl or after exposure to PCB95 (95), 4-OH-PCB95 (4-OH), or 5-OH-PCB95 (5-OH). Mean and SE responses are obtained from $N = 24–70$ myotubes for each treatment recorded from at least 3 separate cultures. $p < .001$ for all 5-OH and 4-OH points relative to Control. PCB95 enhanced responses at low-frequency stimulation ($p < .05$) and depressed at higher frequencies (but did not reach statistical significance). Abbreviations: Caff, caffeine; Ctrl, Control; SR, sarcoplasmic reticulum; TG, thapsigargin.

4-OH-PCB95 caused significant suppression of ECC at all stimulus frequencies tested in those cells remaining responsive; however, 5-OH-PCB95 caused a more pronounced reduction of the Ca^{2+}-transient amplitudes ($p < .001$ comparing 5-OH vs 4-OH at all stimulus frequencies; Figs. 5A [compare right panels] and B [compare triangles vs circles]). Importantly, 5-OH-PCB95 was the only compound to cause a gradual rise in baseline cytoplasmic Ca^{2+}, which led to complete failure of ECC within approximately 10 min in 50% of the cells tested (Table 2), and those cells with measurable responses were dramatically suppressed (Figs. 5A and B). At the end of each experiment, cells were challenged first with 20 mM caffeine and then with 400 nM TG in nominal Ca^{2+}-free external medium to test the responsiveness of RyR1 channels and the filling state of their SR Ca^{2+} stores, respectively (Fig. 5A). These results are summarized in Figure 6. Acute exposure to PCB95 increased responses to caffeine 15% (Fig. 6A) despite a significant (40%) depletion of the SR Ca^{2+} store (Fig. 6B), indicating marked sensitization of RyR1 channels. By contrast, acute exposure to 5-OH- and 4-OH-PCB95 caused a 75% and 50% reduction in the response to caffeine, respectively (Fig. 6A). Subsequent challenge with TG revealed that myotubes exposed to 5-OH-PCB95 had nearly exhausted Ca^{2+} stores, whereas those exposed to 4-OH-PCB95 maintained Ca^{2+} stores similar ($p > .05$) to those of Control (Fig. 6B).

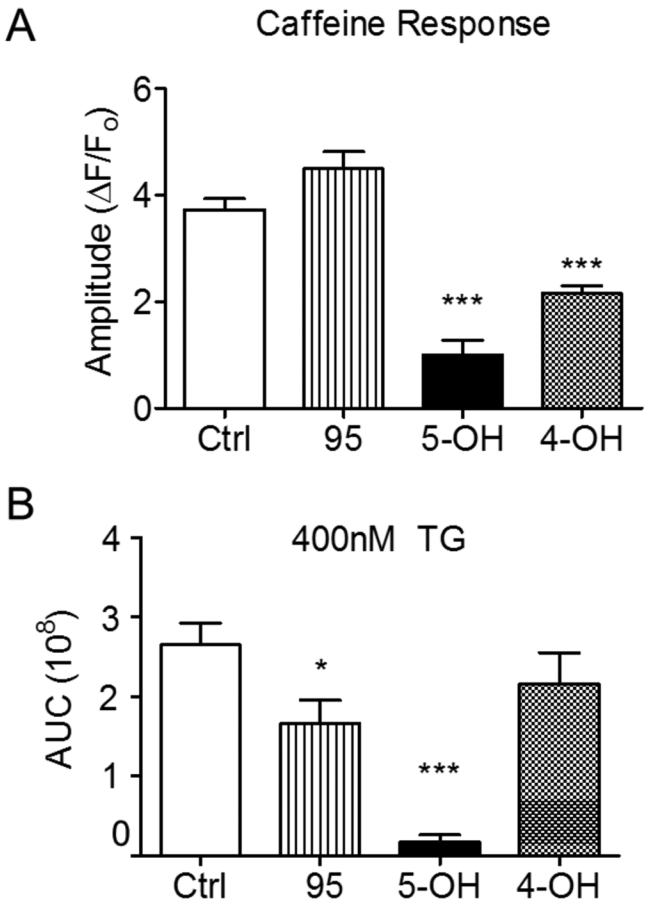

FIG. 6. Caffeine and TG tests of SR Ca^{2+} stores after acute exposure to PCBs. A, Caffeine-sensitive SR Ca^{2+} stores were tested by a challenge to 20 mM Caff. Using this method, PCB95 (5 μM) showed an elevated (though not statistically significant $p = .104$) Ca^{2+} transient compared with control, whereas both 5-OH- and 4-OH-PCB95 elicited significantly attenuated caffeine responses. B, TG (400 nM) was applied to inhibit SERCA actively in the naïve and acutely PCB-treated myotubes to test for SR Ca^{2+} depletion by measuring the AUC for the respective Ca^{2+} transients. PCB95 partially depleted stores, whereas 5-OH–PCB95 fully depleted SR Ca^{2+} stores. 4-OH-PCB95 showed variable depletion of SR stores and the mean did not achieve statistical significance. Error bars represent SEM. $*p < .05$; $***p < .001$, one-way ANOVA with *Dunnett multiple comparison post hoc* test. Abbreviations: AUC, area under the curve; Caff, caffeine; PCB, polychlorinated biphenyl; SR, sarcoplasmic reticulum; TG, thapsigargin.

PCB Substitution Determines Pattern of Subacute Myotube ECC Dysfunction

Before applying the standard pulse train protocol, we documented the fraction of myotubes responding to 1 Hz stimulus train after a 3-h exposure in the presence and absence of PCBs (Fig. 7). Myotubes exposed to 300 nM PCB95 showed a modest decline in fraction of responsive cells that did not reach statistical significance (81% for Control vs 75% for PCB95; $p = .10$). However, 300 nM of either 5-OH-PCB95 or 4-OH-PCB95 produced ECC failure in 81% and 51% of the myotubes, respectively ($p < .001$; Fig. 7).

Nevertheless, the myotubes that retained function after subacute exposure exhibited markedly impaired ECC, and the

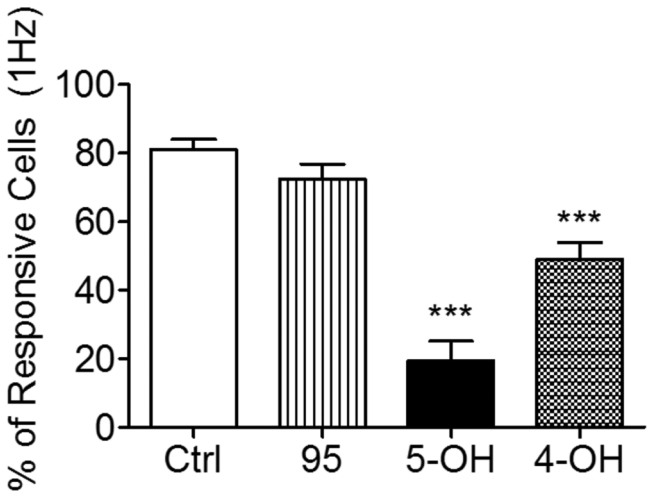

FIG. 7. Subacute exposure to 4-OH- and 5-OH-PCB95 impairs ECC in myotubes. The percent of cells retaining electrically evoked ECC was scored after 3-h exposure to 300 nM vehicle or PCB. Response is defined as the total number of cells responding to a minimum of 1 Hz electrical stimulation within 3–5 fields/well of control and PCB-treated wells within at least 2 different cultures. Fields within each well were chosen randomly, and the ratio of cells responding to total cells was determined. Error bars represent SEM. $***p < .001$; one-way ANOVA with *Dunnett multiple comparison post hoc* test. Abbreviations: ECC, excitation-contraction coupling; PCB, polychlorinated biphenyl.

pattern of dysfunction was dependent on the congener tested (Fig. 8). Subacute exposure to PCB95 resulted in significant depression in ECC across all frequencies tested (Fig. 8A) that was associated with decreased response to caffeine challenge (Fig. 8B). The small fraction of myotubes (19%) retaining ECC responses to 1 Hz stimuli after 3-h exposure to 5-OH-PCB95 showed 2 distinct patterns of activity (Figs. 8C and D; Type 1 and Type 2). Type 1 cells (35% of the cell retaining responses) showed potentiated responses to electrical stimulation between 1 and 2.5 Hz, and completely failed at higher frequencies, whereas Type 2 cells (65% of cell retaining responses) displayed abnormal frequency response profiles compared with control cells across the entire stimulus frequency range ($p < .01$; Fig. 8C). Type 1 cells showed significantly enhanced response to caffeine, whereas Type 2 cells showed caffeine responses modestly greater (but not statistically significant) than control cells (Fig. 8D). All myotubes remaining responsive to 1 Hz stimuli after subacute exposure to 4-OH-PCB95 showed frequency-response profiles similar to the Type 2 phenotype of cells exposed to 5-OH-PCB95 and were significantly different from control at all stimulus frequencies ($p < .001$; Fig. 8E). 4-OH-PCB95-treated myotubes showed significantly ($p < .01$) potentiated responses to caffeine.

DISCUSSION

The rationale for conducting the present investigation is based on: (1) PCBs are known to distribute to striated muscle

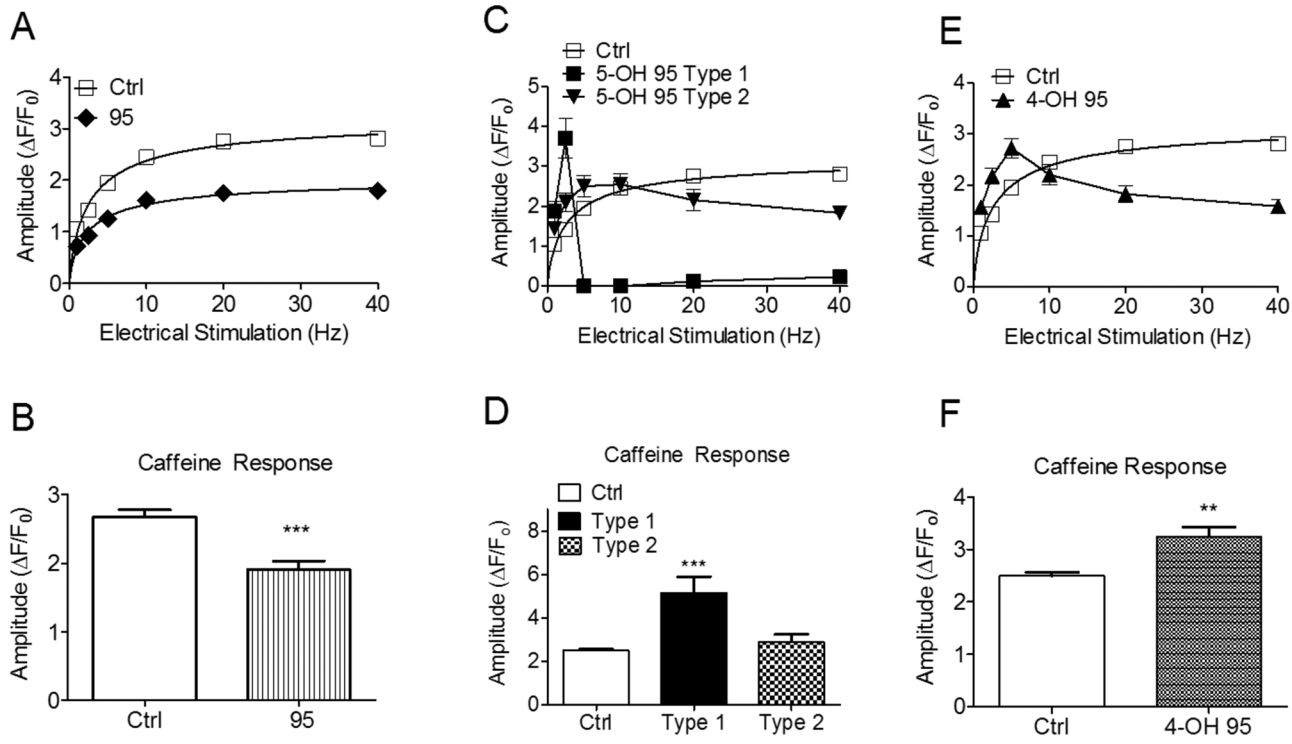

FIG. 8. Differential pattern on ECC dysfunction produced by subacute exposure to PCB95 and its 4-OH and 5-OH derivatives. A, PCB95 (300 nM) suppressed ECC across the entire frequency range tested ($p < .001$ for all points). B, Averaged Ca^{2+} responses elicited by 10-s exposure to 20 mM caffeine showed that subacute PCB95 also produced diminished response compared with control ($p < .001$). C, 5-OH-PCB95 (300nM) elicited 2 types of ECC dysfunction. Type 1 dysfunction produced enhanced responses at low (< 2.5 Hz) stimulus frequencies and complete failure of ECC at ≥ 2.5 Hz. Myotubes exhibiting Type 2 dysfunction responded differently from control at all stimulus frequencies (enhanced at < 5 Hz and suppressed at > 5 Hz [$p < .01$]). D, Responses to caffeine (20mM) in myotubes with Type 1 dysfunction were significantly elevated, whereas cell with Type 2 dysfunction showed a negligible increase ($p > .05$). E, Transient amplitudes of myotubes after exposure to 300 nM 4-OH-PCB95 exhibited responses similar to the fraction of myotubes with Type 2 after subacute exposure to 5-OH-PCB95 ($p < .001$ relative to control across entire frequency range). F, Caffeine response of myotubes after exposure to 4-OH-PCB95 was elevated. All values (excluding 10 Hz) were significantly different from control, $p < .01$. Error bars represent SEM. $^{**}p < .01$; $^{***}p < .001$, one-way ANOVA with *Dunnett multiple comparison post hoc* test. Abbreviation: ECC, excitation-contraction coupling.

(including skeletal muscle), and muscle compartments represent an essential component of PB/PK models of PCB disposition; (2) NDL-PCBs have been demonstrated to directly interact with RyR preparations from striated muscle (skeletal and heart) with concentration-effect curves ranging from nanomolar to low micromolar using biochemical and biophysical methods; however, the functional consequences of such interactions in intact muscle cells has not been investigated; and (3) the SARs for NDL-PCBs and their –OH derivatives for altering fundamental processes in skeletal muscle physiology, ECC, have not been determined. Given that motor impairments can occur indirectly by influencing psychomotor centers of the developing brain and by directly impairing Ca^{2+} dynamics and ECC in developing skeletal muscle, we feel that our new data break novel ground in the field of PCB toxicology. Here we show the first evidence that NDL-PCBs and their OH-metabolites at environmentally relevant concentrations are capable of rapidly and persistently altering Ca^{2+} dynamics and ECC in skeletal myotubes as a consequence of their direct interaction with RyR1 channels. Tight regulation of RyR1 channels within junctional SR of skeletal muscle is essential for not only physiological regulation of muscle contraction and relaxation but also plays an important role in muscle differentiation (Abbott *et al.*, 1998; Jurynec *et al.*, 2008; Valdés *et al.*, 2008; Wu *et al.*, 2011a), and maintaining long-term skeletal muscle health (Andersson *et al.*, 2011; Betzenhauser and Marks, 2010; Kushnir *et al.*, 2010; Pessah *et al.*, 2010). These new mechanistic observations may explain experimental and epidemiological findings that have identified motor impairments as a common feature of PCB exposures. For example, accidental exposures to PCBs in Japan and Taiwan have resulted in protracted motor dysfunction (Fein *et al.,* 1984). Moreover, multiple studies have linked environmental exposures to PCBs to alterations in motor function (Boix *et al.*, 2011; Grandjean *et al.*, 2012; Jacobson *et al.*, 1989; Nishida *et al.*, 1997). The concentrations of NDL-PCBs are higher than DL-PCBs (CDC, 2013). The sum of the major PCBs (ΣPCBs) in human maternal and delivery samples have been reported as high as 230 ng/g lipid (Bergonzi *et al.*, 2011), whereas total PCB levels in the general population are much higher, ranging from 423 to > 1000 ng/g lipid (Wu *et al.*, 2013). Considering the nanomolar potency seen with subacute exposures to PCB95

and its 5-OH-metabolite toward impairing ECC and SR Ca^{2+} dynamics in embryonic muscle, these findings are relevant to current exposure levels and likely to have value in establishing quantitative risk assessments for NDL-PCBs.

A significant, yet unexpected, discovery is that not only does the presence and position of hydroxylation on the phenyl ring dictate the manner in which PCBs and their metabolites modify single RyR1 channel current gating behavior but also the pattern of muscle dysfunction they elicit. All of the NDL-PCB congeners investigated in this study enhanced the binding of [^{3}H]Ry to high-affinity binding sites found in the SR in a concentration-dependent manner. With the steady-state conditions used (3-h incubation), PCB95 and its 5-OH derivative showed the highest potency and efficacy for enhancing [^{3}H]Ry binding of all congeners tested. These results are fully consistent with their ability to rapidly trigger Ca^{2+} release from SR vesicles, even in the presence of SERCA pump activity, which provides strong energy-dependent reaccumulation of Ca^{2+} in opposition to the increased activity of RyR1 channels. The rationale for this conclusion is based on our understanding that the amount of high-affinity [^{3}H]Ry binding detected is a biochemical measure of the degree to which ligands stabilize the RyR1 channel open state (Pessah *et al.*, 1987) and is supported in this study by direct measurements of channel gating kinetics. Single channel analysis clearly indicates that PCB95 (Samsó *et al.*, 2009) and 5-OH-PCB95 (Fig. 3) produce long-lived stability of the full-open channel state. Because PCB95 and 5-OH-PCB95 produce indistinguishable modifications to RyR1 channel gating and SR Ca^{2+} permeability, why these 2 structures produce different patterns of dysfunction in intact myotubes suggests several intriguing insights into how PCBs elicit cellular dysfunction. ECC in skeletal muscle is mediated by a macromolecular complex of interacting proteins, collectively termed the Ca^{2+} release unit (CRU) (Pessah *et al.*, 2010). Two essential components of the CRU are the L-type Ca^{2+} channel CaV1.1 that resides in the T-tubule membrane and RyR1 anchored in the SR that physically interact to tightly regulate each other's function as Ca^{2+} channels. Our current results indicate that PCB95 is highly potent and effective at stabilizing the full-open state of the RyR1 channel, and these effects are consistent with the gradual slow leak of Ca^{2+} form SR stores that ultimately leads to SR Ca^{2+} depletion (Table 3). The predominant consequence of low-level exposure to PCB95 is therefore the attenuated responses to electrically evoked Ca^{2+} transients across the entire range of stimulus frequencies without loss of ECC, which is consistent with a weak uncoupling effect and partial depletion of SR stores with time. Such a pattern of impairment would be expected to weaken muscle contractility and promote fatigability. By contrast, acute challenge with low micromolar 5-OH-PCB95 can promote the rapid and uncontrolled rise in myoplasmic Ca^{2+} associated with near complete depletion of SR Ca^{2+} stores and loss of ECC in a large fraction of myotubes, effects not observed with PCB95. With subacute exposure, nanomolar 5-OH-PCB95 can essentially uncouple ECC in the majority of cells (Fig. 8C) without depletion of SR Ca^{2+} stores or inactivation of RyR1, as evidenced by normal responsiveness to caffeine (Fig. 8D; Table 3). Collectively these results provide the first evidence that 5-OH-PCB95, in addition to being a potent stabilizer of the RyR1 open state, also impairs (uncouples) bidirectional signaling between CaV1.1 and RyR1 that is essential for skeletal muscle ECC. Considering that L-type voltage-dependent Ca^{2+} entry is not necessary to trigger ECC in skeletal muscle, the observation that Ca^{2+} stores are replete and RyR1 remains responsive to caffeine after subacute exposure to 300 nM 5-OH-PCB95 strongly suggests a failure of the CRU to maintain bidirectional signaling. Evidence for nearly identical uncoupling of the CRU of myotubes and adult skeletal fibers has been demonstrated with exposure to the antibacterial triclosan, a NDL-chlorinated diphenyl ether hydroxylated at the 6-position (Cherednichenko *et al.*, 2012). Whether functional uncoupling of orthograde signals between CaV1.1 and RyR1 is an activity that extends to other hydroxylated NDL-PCBs remains to be determined. However, based on the congeners investigated here, hydroxylation at the 4-position is significantly less efficacious in stabilizing the RyR1 open channel state than either the parent compound or the 5-OH derivative. The lower efficacy in stabilizing the open state of individual RyR1 channels can fully explain why 5-OH-PCB95 is incapable of triggering net Ca^{2+} release from SR vesicles in the presence of vigorous SERCA pump activity. It should be emphasized that 4-OH-PCB95 causes unstable modification of gating behavior of RyR1 channels, causing repetitive fluctuations to and from the basal (lower p_o) state, which is likely the result of rapid association/dissociation from of its allosteric modulator site. Such behavior can account for why 4-OH-PCB95 increases binding of [^{3}H]Ry under steady-state conditions (3 h), yet fails to trigger rapid Ca^{2+} release from SR vesicles in the presence of strong SERCA pump activity. 4-OH-PCB95 would be expected to promote [^{3}H]Ry binding in a cumulative manner as the RyR1 channel repeatedly transitions to the open state given that, once bound, [^{3}H]Ry dissociates very slowly thereby acting as a dosimeter of the 4-OH-PCB95 effect over the 3-h incubation. Such unstable enhancement of

TABLE 3
Summary of How PCB95, Its Hydroxylated Derivatives, and Triclosan SR Ca^{2+} Store Content and ECC Uncoupling Under Acute and Subacute Exposures Used in This Study

	5μM Acute		300nM Subacute	
Compound	Uncoupling	Store Depletion	Uncoupling	Store Depletion
95	No	Partial	Weak	Partial
5-OH	Partial	Near complete	Strong	No
4-OH	Weak	No	Moderate	No
Triclosan	Complete	No	Strong[a]	No[a]

Note. [a]Results from Cherednichenko *et al.* (2012) after 24-h exposure to 500nM triclosan.

channel gating, however, is incapable of overcoming the strong SERCA-driven uptake of Ca^{2+} into the vesicles and would be insufficient to trigger net Ca^{2+} release from SR on the short time scale of vesicle experiments. This interpretation is supported by results from intact myotubes that show 4-OH-PCB95 is incapable of depleting SR stores with acute or subacute exposures. Differences in the activity of 4-OH- and 5-OH-PCB95 may be due, at least in part, to the proximity of the acidic hydroxyl to the deactivating –Cl; however, steric hindrance at the 4-position also reduces the potency and efficacy toward RyR1 (Pessah *et al.*, 2006). Regardless, the high activity of NDL-PCBs with 5-OH substitution identified in this study is significant because this represents a major metabolic route in animal studies catalyzed by phenobarbital-inducible CYP450 2B (Kania-Korwel *et al.*, 2012; Wu *et al.*, 2011). Moreover, an important new finding identifies fundamental differences in how PCB derivatives (eg, 4-OH- vs 5-OH-PCB95) modify RyR1 single channel gating behavior and determines the pattern of dysregulation of the entire macroscopic protein complex that comprise the CRU that is responsible for tightly regulating physiological ECC and long-term stability of Ca^{2+} dynamics in the muscle cell.

The current results may also have implications for understanding some of the human health effects reported from human populations exposed to PCBs, especially those associated with motor dysfunction, which have been primarily attributed to developmental neurotoxicity at the level of the CNS (Boix *et al.*, 2011; Schantz *et al.*, 1997). Neurotoxicity of NDL-PCBs has been shown to alter neuronal cell Ca^{2+} homeostasis, dendritic architecture, and activity-dependent plasticity, actions mediated by RyRs (Wayman *et al.*, 2012a,b). Here, we focus on the fidelity of the skeletal muscle as a potential target organ of PCB-mediated motor impairments that may amplify alteration in motor centers in the brain. The pattern of neuromuscular activity is essential for defining skeletal muscle fiber types, maturation of the neuromuscular synapse, and long-term health of skeletal muscle during development (Dayanithi *et al.*, 2006; Ferraro *et al.*, 2012). Moreover, leaky RyR1 channels have been implicated with age-related impairments in ECC, chronic oxidative stress, and loss of muscle function (Gilroy *et al.*, 2012). It should also be emphasized that over 200 mutations in the *RYR1* gene have been associated with malignant hyperthermia (MH) susceptibility whose collective prevalence may be as high as 2% in the general population (Brislin and Theroux, 2013; Pessah *et al.*, 2010). More recently, a few mutations in CaV1.1 have also been shown to confer MH susceptibility (Bannister and Beam, 2013). Thus, interactions between RyR1/CaV1.1 mutations and exposures to NDL-PCB and related compounds may have important gene × environment implications on human health by amplifying muscle dysfunction that impair contractility, enhance fatigue, and promote myopathic changes. Direct impairment of muscle function is possible because striated muscle is a major compartment for the initial disposition of PCBs following exposure (Pessah *et al.*, 2010). A study of Galapagos sea lions identified the congener profile of PCBs found in muscle biopsies (Alava *et al.*, 2009) and that the 10 most active congeners identified based on [^{3}H] Ry-binding analysis (Pessah *et al.*, 2006) represent nearly 25% of the total PCB burden, including 3 of the congeners studied here (PCB95, PCB132, and PCB149). Hints at direct myogenic effects of PCBs have been suggested by previous studies, including inhibition of skeletal muscle differentiation (Coletti *et al.*, 2001), and altered contractility of uterine smooth muscle (Bae *et al.*, 1999a; Bae *et al.*, 1999b) and ventricular cardiomyocytes (Jo *et al.*, 2001).

In conclusion, our studies show the position of hydroxylation of NDL-PCBs dramatically influences how they influence RyR1 channel gating kinetics, SR Ca^{2+} leak, and the pattern of ECC impairment in intact muscle cells (Table 3). Considering the potency of these actions and the implication of RyR1 dysfunction in a number of genetically and environmentally triggered muscle disorders, the direct actions of NDL-PCBs and their hydroxylated metabolites may play a contributing role in motor dysfunction, especially in those individuals with RyR1 mutations (Pessah *et al.* 2010).

FUNDING

National Institutes of Health (NIEHS grants 1R01 ES017425, 1R01 ES014901, P42 ES04699, P42 ES013661); UC Davis Basic and Clinical Communication Science Training Program (T32 DC008072 to Y.N.). The content is solely the responsibility of the authors and does not necessarily represent the official views of the National Institute of Health.

ACKNOWLEDGMENTS

We acknowledge the technical support of Isela Padilla and helpful editing by Rui Zhang and Erika B. Fritsch.

REFERENCES

Abbott, K. L., Friday, B. B., Thaloor, D., Murphy, T. J., and Pavlath, G. K. (1998). Activation and cellular localization of the cyclosporine A-sensitive transcription factor NF-AT in skeletal muscle cells. *Mol. Biol. Cell* **9,** 2905–2916.

Alava, J. J., Ikonomou, M. G., Ross, P. S., Costa, D., Salazar, S., Aurioles-gamboa, D., and Gobas, F. A. (2009). Polychlorinated biphenyls and polybrominated diphenyl ethers in Galapagos sea lions (Zalophus wollebaeki). *Environ. Toxicol. Chem*. **28,** 2271–2282.

Andersson, D. C., Betzenhauser, M. J., Reiken, S., Meli, A. C., Umanskaya, A., Xie, W., Shiomi, T., Zalk, R., Lacampagne, A., and Marks, A. R. (2011). Ryanodine receptor oxidation causes intracellular calcium leak and muscle weakness in aging. *Cell Metab*. **14,** 196–207.

Bae, J., Peters-Golden, M., and Loch-Caruso, R. (1999a). Stimulation of pregnant rat uterine contraction by the polychlorinated biphenyl (PCB) mixture Aroclor 1242 may be mediated by arachidonic acid release through activation of phospholipase A2 enzymes. *J. Pharmacol. Exp. Ther*. **289,** 1112–1120.

Bae, J., Stuenkel, E. L., and Loch-Caruso, R. (1999b). Stimulation of oscillatory uterine contraction by the PCB mixture Aroclor 1242 may involve

increased $[Ca^{2+}]_i$ through voltage-operated calcium channels. *Toxicol. Appl. Pharmacol*. **155,** 261–272.

Bannister, R. A., and Beam, K. G. (2013). Impaired gating of an L-Type Ca(2+) channel carrying a mutation linked to malignant hyperthermia. *Biophys. J*. **104,** 1917–1922.

Bergman, A., Klasson-Wehler, E., and Kuroki, H. (1994). Selective retention of hydroxylated PCB metabolites in blood. *Environ. Health Perspect*. **102,** 464–469.

Bergonzi, R., De Palma, G., Specchia, C., Dinolfo, M., Tomasi, C., Frusca, T., and Apostoli, P. (2011). Persistent organochlorine compounds in fetal and maternal tissues: Evaluation of their potential influence on several indicators of fetal growth and health. *Sci. Total Environ*. **409,** 2888–2893.

Betzenhauser, M. J., and Marks, A. R. (2010). Ryanodine receptor channelopathies. *Pflugers. Arch*. **460,** 467–480.

Bièche, I., Narjoz, C., Asselah, T., Vacher, S., Marcellin, P., Lidereau, R., Beaune, P., and de Waziers, I. (2007). Reverse transcriptase-PCR quantification of mRNA levels from cytochrome (CYP)1, CYP2 and CYP3 families in 22 different human tissues. *Pharmacogenet. Genomics* **17,** 731–742.

Boix, J., Cauli, O., Leslie, H., and Felipo, V. (2011). Differential long-term effects of developmental exposure to polychlorinated biphenyls 52, 138 or 180 on motor activity and neurotransmission. Gender dependence and mechanisms involved. *Neurochem. Int*. **58,** 69–77.

Brislin, R. P., and Theroux, M. C. (2013). Core myopathies and malignant hyperthermia susceptibility: A review. *Paediatr. Anaesth*. **23,** 834–841.

Brooks, S. P., and Storey, K. B. (1992). Bound and determined: A computer program for making buffers of defined ion concentrations. *Anal. Biochem*. **201,** 119–126.

Centers for Disease Control and Prevention (CDC) (2013). Fourth National Report on Human Exposure to Environmental Chemicals. Updated Tables [online]. Available at: http://www.cdc.gov/exposurereport/. Accessed September 9, 2013.

Cherednichenko, G., Ward, C. W., Feng, W., Cabrales, E., Michaelson, L., Samso, M., López, J. R., Allen, P. D., and Pessah, I. N. (2008). Enhanced excitation-coupled calcium entry in myotubes expressing malignant hyperthermia mutation R163C is attenuated by dantrolene. *Mol. Pharmacol*. **73,** 1203–1212.

Cherednichenko, G., Zhang, R., Bannister, R. A., Timofeyev, V., Li, N., Fritsch, E. B., Feng, W., Barrientos, G. C., Schebb, N. H., Hammock, B. D., *et al.* (2012). Triclosan impairs excitation-contraction coupling and Ca^{2+} dynamics in striated muscle. *Proc. Natl. Acad. Sci. U.S.A*. **109,** 14158–14163.

Coletti, D., Palleschi, S., Silvestroni, L., Cannavò, A., Vivarelli, E., Tomei, F., Molinaro, M., and Adamo, S. (2001). Polychlorobiphenyls inhibit skeletal muscle differentiation in culture. *Toxicol. Appl. Pharmacol*. **175,** 226–233.

Dayanithi, G., Mechaly, I., Viero, C., Aptel, H., Alphandery, S., Puech, S., Bancel, F., and Valmier, J. (2006). Intracellular Ca^{2+} regulation in rat motoneurons during development. *Cell Calcium* **39,** 237–246.

DeCaprio, A. P., Johnson, G. W., Tarbell, A. M., Carpenter, D. O., Chiarenzelli, J. R., Morse, G. S., Santiago-Rivera, A. L., and Schymura, M. J.; Akwesasne Task Force on the Environment. (2005). Polychlorinated biphenyl (PCB) exposure assessment by multivariate statistical analysis of serum congener profiles in an adult Native American population. *Environ. Res*. **98,** 284–302.

Ferraro, E., Molinari, F., and Berghella, L. (2012). Molecular control of neuromuscular junction development. *J. Cachexia. Sarcopenia Muscle* **3,** 13–23.

Gilroy, E. A., McMaster, M. E., Parrott, J. L., Hewitt, L. M., Park, B. J., Brown, S. B., and Sherry, J. P. (2012). Assessment of the health status of wild fish from the Wheatley Harbour Area of Concern, Ontario, Canada. *Environ. Toxicol. Chem*. **31,** 2798–2811.

Grandjean, P., Weihe, P., Nielsen, F., Heinzow, B., Debes, F., and Budtz-Jørgensen, E. (2012). Neurobehavioral deficits at age 7 years associated with prenatal exposure to toxicants from maternal seafood diet. *Neurotoxicol. Teratol*. **34,** 466–472.

Guo, Y. L., Chen, Y. C., Yu, M. L., and Hsu, C. C. (1994). Early development of Yu-Cheng children born seven to twelve years after the Taiwan PCB outbreak. *Chemosphere* **29,** 2395–2404.

Hovander, L., Malmberg, T., Athanasiadou, M., Athanassiadis, I., Rahm, S., Bergman, A., and Wehler, E. K. (2002). Identification of hydroxylated PCB metabolites and other phenolic halogenated pollutants in human blood plasma. *Arch. Environ. Contam. Toxicol*. **42,** 105–117.

Hu, D., and Hornbuckle, K. C. (2010). Inadvertent polychlorinated biphenyls in commercial paint pigments. *Environ. Sci. Technol*. **44,** 2822–2827.

Jacobson, J. L., Humphrey, H. E., Jacobson, S. W., Schantz, S. L., Mullin, M. D., and Welch, R. (1989). Determinants of polychlorinated biphenyls (PCBs), polybrominated biphenyls (PBBs), and dichlorodiphenyl trichloroethane (DDT) levels in the sera of young children. *Am. J. Public Health* **79,** 1401–1404.

Jo, S. H., Choi, S. Y., Kim, K. T., and Lee, C. O. (2001). Effects of polychlorinated biphenyl 19 (2,2',6-trichlorobiphenyl) on contraction, Ca^{2+} transient, and Ca^{2+} current of cardiac myocytes. *J. Cardiovasc. Pharmacol*. **38,** 11–20.

Joshi, S. N., Vyas, S. M., Duffel, M. W., Parkin, S., Lehmler, H. J. (2011). Synthesis of Sterically Hindered Polychlorinated Biphenyl Derivatives. *Synthesis (Stuttg)*. **7,** 1045–1054.

Jurynec, M. J., Xia, R., Mackrill, J. J., Gunther, D., Crawford, T., Flanigan, K. M., Abramson, J. J., Howard, M. T., and Grunwald, D. J. (2008). Selenoprotein N is required for ryanodine receptor calcium release channel activity in human and zebrafish muscle. *Proc. Natl. Acad. Sci. U.S.A*. **105,** 12485–12490.

Kania-Korwel, I., Barnhart, C. D., Stamou, M., Truong, K. M., El-Komy, M. H., Lein, P. J., Veng-Pedersen, P., and Lehmler, H. J. (2012). 2,2',3,5',6-Pentachlorobiphenyl (PCB 95) and its hydroxylated metabolites are enantiomerically enriched in female mice. *Environ. Sci. Technol*. **46,** 11393–11401.

Kania-Korwel, I., Shaikh, N. S., Hornbuckle, K. C., Robertson, L. W., and Lehmler, H. J. (2007). Enantioselective disposition of PCB 136 (2,2',3,3',6,6'-hexachlorobiphenyl) in C57BL/6 mice after oral and intraperitoneal administration. *Chirality* **19,** 56–66.

Kenet, T., Froemke, R. C., Schreiner, C. E., Pessah, I. N., and Merzenich, M. M. (2007). Perinatal exposure to a noncoplanar polychlorinated biphenyl alters tonotopy, receptive fields, and plasticity in rat primary auditory cortex. *Proc. Natl. Acad. Sci. U.S.A*. **104,** 7646–7651.

Kostyniak, P. J., Hansen, L. G., Widholm, J. J., Fitzpatrick, R. D., Olson, J. R., Helferich, J. L., Kim, K. H., Sable, H. J., Seegal, R. F., Pessah, I. N., *et al.* (2005). Formulation and characterization of an experimental PCB mixture designed to mimic human exposure from contaminated fish. *Toxicol. Sci*. **88,** 400–411.

Kushnir, A., Betzenhauser, M. J., and Marks, A. R. (2010). Ryanodine receptor studies using genetically engineered mice. *FEBS Lett*. **584,** 1956–1965.

Larsson, C., Ellerichmann, T., Hühnerfuss, H., and Bergman, A. (2002). Chiral PCB methyl sulfones in rat tissues after exposure to technical PCBs. *Environ. Sci. Technol*. **36,** 2833–2838.

Lehmler, H. J., Harrad, S. J., Hühnerfuss, H., Kania-Korwel, I., Lee, C. M., Lu, Z., and Wong, C. S. (2010). Chiral polychlorinated biphenyl transport, metabolism, and distribution: A review. *Environ. Sci. Technol*. **44,** 2757–2766.

Marek, R. F., Thorne, P. S., Wang, K., Dewall, J., Hornbuckle, K. C. (2013). PCBs and OH-PCBs in serum from children and mothers in urban and rural U.S. communities. *Environ Sci Technol*. **47,** 3353–3361.

Martinez, A., Erdman, N. R., Rodenburg, Z. L., Eastling, P. M., and Hornbuckle, K. C. (2012). Spatial distribution of chlordanes and PCB congeners in soil in Cedar Rapids, Iowa, USA. *Environ. Pollut*. **161,** 222–228.

Martinez, A., and Hornbuckle, K. C. (2011). Record of PCB congeners, sorbents and potential toxicity in core samples in Indiana Harbor and Ship Canal. *Chemosphere* **85,** 542–547.

Nakai, J., Dirksen, R. T., Nguyen, H. T., Pessah, I. N., Beam, K. G., and Allen, P. D. (1996). Enhanced dihydropyridine receptor channel activity in the presence of ryanodine receptor. *Nature* **380,** 72–75.

Nishida, N., Farmer, J. D., Kodavanti, P. R., Tilson, H. A., and MacPhail, R. C. (1997). Effects of acute and repeated exposures to Aroclor 1254 in adult rats: Motor activity and flavor aversion conditioning. *Fundam. Appl. Toxicol*. **40,** 68–74.

Pessah, I. N., Cherednichenko, G., and Lein, P. J. (2010). Minding the calcium store: Ryanodine receptor activation as a convergent mechanism of PCB toxicity. *Pharmacol. Ther*. **125,** 260–285.

Pessah, I. N., Hansen, L. G., Albertson, T. E., Garner, C. E., Ta, T. A., Do, Z., Kim, K. H., and Wong, P. W. (2006). Structure-activity relationship for non-coplanar polychlorinated biphenyl congeners toward the ryanodine receptor-Ca^{2+} channel complex type 1 (RyR1). *Chem. Res. Toxicol*. **19,** 92–101.

Pessah, I. N., Lehmler, H. J., Robertson, L. W., Perez, C. F., Cabrales, E., Bose, D. D., and Feng, W. (2009). Enantiomeric specificity of (-)-2,2',3,3',6,6'-hexachlorobiphenyl toward ryanodine receptor types 1 and 2. *Chem. Res. Toxicol*. **22,** 201–207.

Pessah, I. N., Stambuk, R. A., and Casida, J. E. (1987). Ca^{2+}-activated ryanodine binding: Mechanisms of sensitivity and intensity modulation by Mg^{2+}, caffeine, and adenine nucleotides. *Mol. Pharmacol*. **31,** 232–238.

Saito, A., Seiler, S., Chu, A., and Fleischer, S. (1984). Preparation and morphology of sarcoplasmic reticulum terminal cisternae from rabbit skeletal muscle. *J. Cell Biol*. **99,** 875–885.

Samsó, M., Feng, W., Pessah, I. N., and Allen, P. D. (2009). Coordinated movement of cytoplasmic and transmembrane domains of RyR1 upon gating. *PLoS Biol*. **7,** e85.

Schantz, S. L., Seo, B. W., Wong, P. W., and Pessah, I. N. (1997). Long-term effects of developmental exposure to 2,2',3,5',6-pentachlorobiphenyl (PCB 95) on locomotor activity, spatial learning and memory and brain ryanodine binding. *Neurotoxicology* **18,** 457–467.

Song, E. Q., Ma, X. Y., Tian, X. G., Liu, J., Liu, L. C., Dong, H., and Song, Y. (2013). The effect of the structure of polychlorinated biphenyls on their hydroxylation, oxidation, and glutathionyl conjugation reactions. *Biomed. Environ. Sci*. **26,** 138–147.

Tanabe, T., Beam, K. G., Powell, J. A., and Numa, S. (1988). Restoration of excitation-contraction coupling and slow calcium current in dysgenic muscle by dihydropyridine receptor complementary DNA. *Nature* **336,** 134–139.

Thomas, K., Xue, J., Williams, R., Jones, P., and Whitaker, D. (2012). *Polychlorinated Biphenyls (PCBs) in School Buildings: Sources, Environmental Levels, and Exposures*. Office of Research and Development, Nat Exp Res Lab, Durham, NC.

Valdés, J. A., Gaggero, E., Hidalgo, J., Leal, N., Jaimovich, E., and Carrasco, M. A. (2008). NFAT activation by membrane potential follows a calcium pathway distinct from other activity-related transcription factors in skeletal muscle cells. *Am. J. Physiol. Cell Physiol*. **294,** C715–C725.

Warner, N. A., Martin, J. W., and Wong, C. S. (2009). Chiral polychlorinated biphenyls are biotransformed enantioselectively by mammalian cytochrome P-450 isozymes to form hydroxylated metabolites. *Environ. Sci. Technol*. **43,** 114–121.

Wayman, G. A., Bose, D. D., Yang, D., Lesiak, A., Bruun, D., Impey, S., Ledoux, V., Pessah, I. N., and Lein, P. J. (2012a). PCB-95 modulates the calcium-dependent signaling pathway responsible for activity-dependent dendritic growth. *Environ. Health Perspect*. **120,** 1003–1009.

Wayman, G. A., Yang, D., Bose, D. D., Lesiak, A., Ledoux, V., Bruun, D., Pessah, I. N., and Lein, P. J. (2012b). PCB-95 promotes dendritic growth via ryanodine receptor-dependent mechanisms. *Environ. Health Perspect*. **120,** 997–1002.

Wu, H., Bertrand, K. A., Choi, A. L., Hu, F. B., Laden, F., Grandjean, P., and Sun, Q. (2013). Persistent organic pollutants and type 2 diabetes: A prospective analysis in the nurses' health study and meta-analysis. *Environ. Health Perspect*. **121,** 153–161.

Wu, H. H., Brennan, C., and Ashworth, R. (2011). Ryanodine receptors, a family of intracellular calcium ion channels, are expressed throughout early vertebrate development. *BMC Res. Notes* **4,** 541.

Wu, X., Pramanik, A., Duffel, M. W., Hrycay, E. G., Bandiera, S. M., Lehmler, H. J., and Kania-Korwel, I. (2011). 2,2',3,3',6,6'-Hexachlorobiphenyl (PCB 136) is enantioselectively oxidized to hydroxylated metabolites by rat liver microsomes. *Chem. Res. Toxicol*. **24,** 2249–2257.

Yang, D., Kim, K. H., Phimister, A., Bachstetter, A. D., Ward, T. R., Stackman, R. W., Mervis, R. F., Wisniewski, A. B., Klein, S. L., Kodavanti, P. R., *et al.* (2009). Developmental exposure to polychlorinated biphenyls interferes with experience-dependent dendritic plasticity and ryanodine receptor expression in weanling rats. *Environ. Health Perspect*. **117,** 426–435.